Terra and Aqua MODIS Thermal Emissive Bands calibration and RVS stability assessments using an in situ ocean target

Carlos L. Pérez Díaz, Xiaoxiong Xiong, Aisheng Wu, and Tiejun Chang

***Abstract*—MODIS, whose openly-public data have been used for over two decades to monitor and address global issues, has 16 Thermal Emissive Bands (TEBs) with central wavelengths that range from 3.7 μm to 14.4 μm, and are calibrated on-orbit using observations from its on-board blackbody. In order to maintain MODIS' rich, well-calibrated archive of multispectral imagery and data, Earth targets are regularly used to track its long-term stability, as well as the consistency between the two sensors onboard the Terra and Aqua satellites. Moreover, these scenes can be used to compare MODIS Earth view data over the complete scan-angle range and evaluate the on-orbit performance of the TEBs response-versus-scan-angle (RVS) over mission lifetime. This manuscript focuses on evaluating the MODIS TEBs Collection (C6.1) radiometric calibration stability for both instruments using an in situ ocean target as reference (hereafter referred to as in situ sea surface temperature (SST)). Furthermore, it will assess the calibration consistency between the MODIS sensors. Lastly, it will analyze the on-orbit RVS stability for Terra and Aqua MODIS. Only cloud-free, nighttime MODIS TEB retrievals were used for the study. A normalization methodology is applied to standardize the MODIS data to the in situ SST. Additionally, spectral corrections were derived between some of the Terra and Aqua MODIS TEBs by using a combination of the MODIS Atmospheric Profile product and MODerate resolution atmospheric TRANsmission (MODTRAN) simulations. Results indicate that most MODIS TEBs exhibit mission-long trends of ±0.50 K – with Terra band 30 presenting the largest downward drift due to residual electronic cross-talk effects. Moreover, the calibration consistency analysis over a warm ocean target demonstrated that the average Terra-to-Aqua MODIS bias for most bands is well within ±0.50 K (bands 27 and 30 show the largest - electronic crosstalk-related - biases). Lastly, the MODIS TEBs RVS trends display changes of ±0.50 K (except for bands 25 and 27 at the end-of-scan angles) for both instruments. Overall, the MODIS TEBs remain well-calibrated and their RVSs aptly-characterized.**

***Index Terms*— MODIS, thermal emissive bands, calibration, RVS**

I. Introduction

THE Moderate Resolution Imaging Spectroradiometer (MODIS) is a fundamental instrument for The National Aeronautics and Space Administration (NASA) Earth Observing System (EOS). Presently, two MODIS instruments operate in-orbit onboard the Terra and Aqua spacecraft. Over their lifetimes (20 and 18 years for Terra and Aqua, correspondingly), both instruments have provided nearly-continuous Earth observations that have contributed significantly to land, oceanic, and atmospheric studies. MODIS is a cross-track scanning radiometer that employs a two-sided mirror and records observations in 36 spectral bands, 16 of which are Thermal Emissive Bands (TEBs) whose central wavelengths range from 3.7 μm to 14.4 μm and have a 1-km spatial resolution at nadir. The MODIS TEBs use a quadratic calibration algorithm that is applied to on-orbit observations from a temperature-controlled flat-panel v-groove blackbody (BB) on a scan-by-scan basis, and whose calibration coefficients are updated using the BB's response [1]. On-board BB warm-up and cooldown (WUCD) operations, BB temperature goes from ambient to 315 K, are performed quarterly to derive the MODIS TEBs non-linear (a_0 and a_2) calibration coefficients. Thus, on-orbit calibration updates are essential to track the instrument response changes and maintain high product quality.

MODIS has a double-sided mirror. Each mirror side scan produces a 10 km (at nadir) by 2330 km swath for each TEB. All Earth-view (EV) retrievals are acquired over a mirror side angle range of ±55 degrees that corresponds to an angle-of-incidence (AOI) spanning from 10.65 to 65.5 degrees. System level response-versus-scan-angle (RVS) is a fundamental calibration parameter for remote sensing radiometers making observations via optical scanning systems (e.g. scan mirror). Generally, a sensor's on-orbit calibration is performed at a fixed viewing angle, while the EV scene observations are made continuously over a wider range geometry. Thus, the response of all sensors with optical scanning systems is scan angle reliant. Hence, well-informed insight of any possible RVS dependency is crucial for the calibration of MODIS science data [2].

Terra MODIS Collection (C6.1) includes the implementation of the photovoltaic (PV) longwave infrared (LWIR) bands 27-

C. L. Pérez Díaz is with Science Systems and Applications, Inc., Lanham, MD 20706 USA (e-mail: carlos.perez@ssaihq.com).

X. Xiong is with the Sciences and Exploration Directorate, NASA/GSFC, Greenbelt, MD 20771 USA (e-mail: xiaoxiong.xiong-1@nasa.gov).

A. Wu is with Science Systems and Applications, Inc., Lanham, MD 20706 USA (e-mail: aisheng.wu@ssaihq.com).

T. Chang is with Science Systems and Applications, Inc., Lanham, MD 20706 USA (e-mail: tiejun.chang@ssaihq.com).

30 electronic cross-talk correction. Signal contamination levels early in the Terra MODIS mission were relatively low; and thus, the correction impact was minor as well. However, after the February 2016 Terra safe mode event, the signal contamination for each PV LWIR band increased drastically, as did its impact on several L1B products. Hence, in order to characterize and correct the electronic cross-talk signal contamination, monthly Moon observations have been used to derive suitable correction coefficients to apply to the detector's digital response for the aforementioned Terra MODIS TEBs. Applying the correction throughout the Terra MODIS mission for C6.1 resulted in an improvement to both the image quality and long-term radiometry when compared to Collection 6 [3], [4]. Additionally, an update in the C6.1 procedure starting from January 2019 was established where, after every Terra MODIS lunar roll maneuver and subsequent PV LWIR TEBs cross-talk coefficients derivation, the a_0 and a_2 calibration coefficients are generated using the newly-created PV LWIR cross-talk coefficients and last BB WUCD data. This procedure change was incorporated due to current rapid electronic cross-talk changes after the safe mode event. It was deemed necessary because otherwise the delivered a_0 and a_2 calibration coefficients would always be lagging for these four TEBs, as the BB WUCD operations are performed quarterly and cross-talk is continually changing. MODIS C6.1 was used for this study.

Vicarious calibration practices are commonly used as an alternative to the onboard calibration techniques for sensor performance monitoring. As such, Earth scene observations provide useful information for calibration assessments. In the past, the radiometric calibration of the TEBs has been evaluated for C6.1 using Infrared Atmospheric Sounding Interferometer (IASI) Simultaneous Nadir Overpasses (SNOs) and Himawari-8/ Advanced Himawari Imager (AHI) data as warm references [5],[6]. However, the MODIS C6.1 TEBs have not been evaluated for calibration stability using in situ SST. Some additional C6.1 calibration stability studies were performed for cold scenes by assessing the MODIS LWIR PV bands 27-30 and window channels (bands 31 and 32) using Dome Concordia (Dome-C) as proxy, as well as deep convective clouds as reference [7]-[9].

After the Terra MODIS TEBs RVSs were successfully characterized on-orbit, both the Terra and Aqua MODIS TEBs RVSs have been recurrently monitored for subsequent Collections [10]. Preceding studies for prior Collections have: used observations made during a MODIS data sector rotation throughout a lunar observation, used the MODIS EV brightness temperatures (BTs) over the North Atlantic Ocean, and considered three different methods (MODIS EV BTs minus in situ SST, MODIS EV BTs, and digital response over the full swath width) to evaluate the on-orbit MODIS TEBs RVSs over Dome-C and the North Atlantic Ocean [11]-[13]. However, only two studies have evaluated the RVS stability of the MODIS TEBs for C6.1, albeit for cold scenes or using spacecraft maneuvers. The former assessed the on-orbit MODIS TEBs RVS stability by comparing the MODIS EV BTs at different AOIs using Dome-C (cold scene), while the latter evaluated the MODIS TEBs on-orbit RVS calibration and characterization using observations from spacecraft pitch maneuvers [14],[15].

This study focuses on the MODIS TEBs calibration and consistency assessments using an in situ SST (buoy located in the Pacific Ocean near Sand Island in Hawaii). The mission-long calibration and RVS characterization stability and consistency between Terra and Aqua MODIS are assessed. Common artifacts when using Earth scene measurements are seasonal variations and scene-associated non-uniformity. Normalizing the satellite data to in situ SST can remove these variations. The technique used in this work combines the empirical modeling of the relationship between a band and in situ SST to normalize the data [16]. In this manuscript, the MODIS data is standardized to the in situ SST prior to the MODIS TEBs calibration assessments. Additionally, because it is known that there are spectral differences between some Terra and Aqua MODIS bands, a spectral correction was derived using a combination of the MODIS Atmospheric Profile products and MODerate resolution atmospheric TRANsmission (MODTRAN) simulations. Cloud-covered granules, as defined by the MODIS cloud mask products, were excluded from the analyses.

Section II briefly describes the MODIS TEBs RVSs characterization and calibration algorithm background, as well as presents a description of the in situ ocean site and its surface temperature measurements and the MODIS products used in this study. Section III discusses the methodology employed; which mainly consists of an in-detail description on how to normalize the MODIS data to the in situ SST and the spectral correction derivation. Section IV examines the results by means of calibration stability and consistency assessments for all the MODIS TEBs and both instruments. Lastly, Section V presents our conclusion based on the findings of this paper.

II. Background

A. MODIS TEBs RVSs characterization

Response-versus-scan angle characterization is a significant feature of pre-launch testing. Because the Terra pre-launch RVS characterization was not performed properly, a series of on-orbit deep space pitch maneuvers (DSM) were executed on the spacecraft in early 2003 to derive its TEBs RVSs [10],[15]. A spacecraft deep space pitch maneuver is a designated post-launch activity for TEB RVS characterization. Present-day Terra MODIS Level-1 (L1B) data production uses the TEBs RVSs resulting from the DSM. Moreover, the setbacks experienced and lessons learned during the Terra pre-launch RVS characterization were instrumental for the application of an accurate and thorough Aqua MODIS RVS categorization under different operational configurations during pre-launch. In summary, the RVS for both instruments were derived during pre-launch. However, the pre-launch Terra MODIS RVS were not characterized correctly and had to be derived again post-launch using data from a DSM. Those (post-launch-derived) are the Terra MODIS RVS values currently used and shown in Fig. 1. The Aqua MODIS RVS were derived correctly during pre-

launch and are shown in Fig. 1 as well. Edge-of-frame angles exhibit the largest RVS differences - when compared to the BB viewing angle.

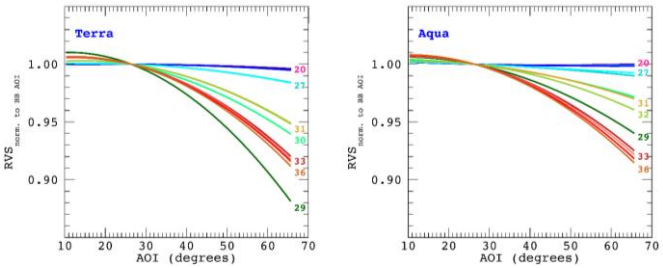

Fig. 1. Terra and Aqua MODIS TEBs RVSs normalized to BB AOI (26.7°).

B. *MODIS TEBs calibration algorithm*

The MODIS TEBs include mid-wave infrared (MWIR) bands 20-25 and LWIR bands 27-36. Bands 20-30 consist of ten PV detectors per band, while bands 31-36 consist of ten photo-conductive (PC) detectors per channel. All TEB detectors are located on two cold focal plane assemblies (CFPAs): a short-wave and mid-wave infrared (SMWIR) FPA and a LWIR FPA, which are nominally controlled on-orbit at 83 K. The on-board BB serves as the primary calibration source, while the space view (SV) provides a reference for the instrument background. The MODIS TEBs calibration uses a quadratic algorithm on a scan-by-scan basis for each TEB detector and side of the scan mirror. The BB WUCD operation, with a variant temperature ranging from instrument ambient (about 270 K) to 315 K, is used to characterize the instrument's on-orbit non-linear response coefficients. During nominal operation, the BB temperature is set to 290 K and 285 K for Terra and Aqua MODIS, respectively, and the response function's linear coefficient is calibrated scan-by-scan for each TEB, whereas the non-linear terms are obtained from a look-up table [17],[18].

The MODIS TEBs quadratic calibration algorithm converts the sensor's digital response to calibration radiance (L_{cal}). The BB calibration radiance itself is adjusted for instrument self-emission due to RVS effects,

$$L_{cal} = RVS_{BB} \cdot \varepsilon_{BB} \cdot L_{BB} + (RVS_{SV} - RVS_{BB}) \cdot L_{SM} + RVS_{BB} \cdot (1 - \varepsilon_{BB}) \cdot \varepsilon_{CAV} \cdot L_{CAV}, \quad (1)$$

where RVS_{BB} and RVS_{SV} are the RVSs at the BB and SV AOIs, L_{BB}, L_{SM}, L_{CAV} are the BB, scan mirror, and cavity radiances, and ε_{BB} and ε_{CAV} are the BB and cavity emissivities. A quadratic function, $L_{cal} = a_0 + b_1 dn_{BB} + a_2 dn_{BB}^2$, is used for instrument response calibration by means of an offset term, a_0, a quadratic term, a_2, and the BB digital response given in digital counts (dn_{BB}). Thus, the linear calibration coefficient for Earth radiance retrievals can be articulated as:

$$b_1 = [RVS_{BB}\varepsilon_{BB}L_{BB} + (RVS_{SV} - RVS_{BB})L_{SM} + RVS_{BB}(1 - \varepsilon_{BB})\varepsilon_{cav}L_{CAV} - a_0 - a_2 dn_{BB}^2]/dn_{BB}. \quad (2)$$

The current TEB calibration algorithm only uses the cooldown portion of the BB WUCD operation to derive the offset and non-linear calibration coefficients. Previous literature by Xiong *et al.*, Chiang *et al.*, and Guenther *et al.*, have provided detailed descriptions of the MODIS TEB pre-launch and on-orbit calibration algorithms, and uncertainty analyses [1],[19],[20]. An extension to the MODIS TEBs calibration algorithm information presented in this paper can be found on the MODIS L1B Algorithm Theoretical Basis Document [21].

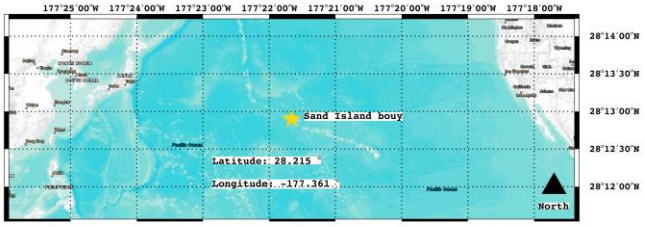

Fig. 2. Location of the NBDC buoy used as the in situ ocean target for this study. (Map source: openstreetmap.org).

C. *In situ ocean target*

The in situ ocean target site selected for this study belongs to the National Water Level Observation Network (NWLON). Figure 2 depicts the geographical location of the station. The site is operated and maintained by the National Oceanic and Atmospheric Administration's National Data Buoy Center (NOAA's NDBC). This target was chosen both due to its contribution to the NDBC Moored Buoy program and continuous operation - few to no data outages - for most of the on-orbit MODIS lifetime. The ocean buoy site is commonly known as Station SNDP5 (or #1619910), and is positioned near the Sand Island, Midway Islands, HI (28.215 N, 177.361 W). The buoy is a 3-meter discus buoy with a standard Self-Contained Ocean Observing Payload (SCOOP) of sensors. The measurements are made at the Mean Lower Low Water level with high-accuracy (± 0.002 °C) inductive instruments from Sea-Bird Electronics (SBE) currently used by the NDBC for climate-quality observations. The inductive sensors include a mix of: three SBE-39 temperature sensors, three SBE-39 temperature and pressure sensors, and three SBE-37 conductivity, temperature, and pressure sensors. The SST data demonstrate excellent long-term stability with a trend of 0.0001 K/yr. The data have been recorded every 6 minutes since 2005. Major data gaps include: 7 months in 2005, 5 months in 2010, 2 months in 2014, and 2 months in 2019. All data and additional details are available via the NDBC website [22].

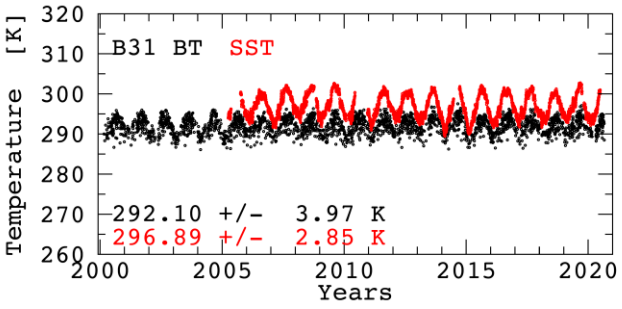

Fig. 3. Terra MODIS band 31 nighttime BT and ocean buoy SST times series.

Figure 3 illustrates the Terra MODIS band 31 nighttime BT and ocean buoy sea surface temperature (SST) time series. A cross-comparison between these datasets indicates that the band 31 BTs and ocean SSTs are quite similar with average values and standard deviations of 292.10 K and 3.97 K and 296.89 K and 2.85 K, respectively. This is a good, albeit preliminary indication that the normalization method can be successfully applied using the SST data record. The application will be described in detail in Section IV.

D. MODIS products

MODIS C6.1 L1B calibrated radiance, geolocation, cloud mask, and atmospheric profile products were downloaded for the granules coincident with the selected target to extract the necessary radiance, location, cloud cover, and atmospheric profile information for the analysis, respectively. There are roughly four MODIS overpasses per day over the selected site. Only nighttime granules were used for the analyses to avoid the solar reflectance impacts on the MWIR bands. Cloud-covered pixels, as flagged by the MODIS cloud mask, were filtered out.

Prior to employing the methods discussed in Section III, a 400 km^2 (20 km x 20 km) region-of-interest (ROI) – centered around the ocean buoy site – was located using the great-circle distance. The MODIS L1B calibrated radiance data were then converted to BTs for all TEBs and all 400 pixels using each band's spectral response function and Planck's law. Afterwards, all cloud-covered pixels, as identified by the cloud mask, were filtered out, and the average BT of the remaining pixels was calculated. Only those pixels with "probably clear" or "confident clear" flag designations were considered. Data from all (including those categorized as noisy) 10 detectors for all TEBs were used to calculate the band-averaged BTs. Inoperable detectors (currently or in the past) for any Terra and Aqua MODIS TEB were excluded from the mean BT calculation. Lastly, all in situ SST were matched temporally – to the nearest 6th minute – with the coincident MODIS overpass.

III. Methodology Development

A. MODIS data normalization using in situ SST

As proven in previous studies, reference temperature measurements can be used to track the on-orbit calibration stability and consistency of the Terra and Aqua MODIS TEBs [6],[8],[9]. In this work, a normalization technique is used for the TEBs calibration assessments using an ocean target. Sensor measurements can be referenced to those from an in situ target or a well-calibrated band [16]. In order to improve the accuracy of the calibration assessments, the MODIS measurements are normalized to the reference's temperatures. This normalized temperature can be selected as the average temperature of the reference measurements, or a key temperature feasible for calibration assessments. Usually, the EV retrievals from any given band have some degree of correlation with reference measurements over an Earth scene. This affiliation can be derived using a physical or empirical model. In this case, an empirical model is used to describe the relationship between band and reference (in situ) measurements. Both the correlation and normalization can be combined as follows:

$$BT_{model}(b) = f\left(BT_{ref} - BT_{ref_{nor}}\right), \quad (3)$$

where BT_{ref} are the reference measurements, and $BT_{ref_{nor}}$ is the normalization temperature of the reference measurements. Naturally, this dependency function should be determined from various tests over an Earth scene. In this work, the in situ SST or MODIS band 31 BTs are used as references for the stability assessment of all TEB. Both the in situ SST and band 31 BTs have distributions that vary monthly and yearly. These fluctuations can impact the calibration assessment's accuracy and consistency. Hence, because the in situ SST (or band 31 BTs) distribution varies significantly, this work provides a method to normalize the other bands BTs to the reference source (in situ SST or band 31 BTs). Thus, these affinities can be used for the development of an empirical model to normalize all other TEB BTs to a reference temperature (i.e. in situ SST or MODIS band 31 BTs) to enhance the assessment's accuracy. Because the in situ SST or band 31 BTs distributions can have reasonably large spreads over ocean, a reference temperature is defined for normalization, and the following empirical model (a quadratic function) is developed,

$$BT_{model}(b) = c_0 + c_1\left(BT_{ref} - BT_{ref_{nor}}\right) + c_2\left(BT_{ref} - BT_{ref_{nor}}\right)^2, \quad (4)$$

where $c_{0,1,2}$ are fitting coefficients and $BT_{ref_{nor}}$, the normalization temperature, is designated as 292 K and 296 K for band 31 and the in situ SST, respectively. The fitting coefficients are determined from the model regression dependency (Fig. 7). The c_0 fitting coefficient is the TEB's normalized ocean BT to the in situ SST or band 31 at the reference BT. The fitting coefficients can then be used to obtain the BT distribution after normalization as such:

$$BT_{nor}(b) = BT(b) - c_1\left(BT_{ref} - BT_{ref_{nor}}\right) - c_2\left(BT_{ref} - BT_{ref_{nor}}\right)^2 . \quad (5)$$

The method relies on establishing reasonable relationship between the band and in situ SST over the selected scene. Thus, the calibration assessment's accuracy will depend on the correlation between these measurements. Hence, this method may not work for a band with low correlation with its reference. Meaning that the model is not able to fully capture the fluctuations and normalize the data (to remove its seasonality) for these bands using the in situ SST. This will be discussed in detail in Section III.B. Nonetheless, the technique's goal is to provide betterment to the assessment's accuracy, and therefore calibration assessments at the desired signal levels. In order to do this, the band's BT (e.g. typical or average temperature over the scene) is selected, and its corresponding in situ SST is calculated from the empirical model. Afterwards, the in situ SST is used as the reference BT.

B. In situ and satellite data cross-comparison considerations

There are significant differences between in situ measurements and satellite instrument (e.g. MODIS) retrievals. Firstly, the top-of-atmosphere measurements from satellite instruments are affected by both the atmosphere and cloud conditions - even for those bands designed for Earth surface BT retrievals. Secondly, satellite instruments measure spectral radiance, and then convert to BT for the corresponding band wavelength spectra. Hence, the scene emissivity is spectrally-dependent, and makes the in situ SST and satellite instrument BTs different. Lastly, scene uniformity, seasonal variation, and time difference between measurements have effects on the satellite instrument retrievals. On the other hand, in situ measurements have distinctive advantages such as: precise and accurate instrument calibration and SI traceability. Moreover, in situ measurements make it possible to monitor climate change effects when evaluating the calibration performance of satellite data if the two datasets diverge significantly. However, that's not to say that measurements from other spectral bands do not carry some advantages such as: same pixel measurements over near identical geolocations, simultaneous measurements, and a similar calibration algorithm. Furthermore, an instrument's band specifications vary with the design and application. For instance, MODIS band 31 (11-μm; primarily used for surface and cloud temperature retrievals) has the stringiest requirement of all the MODIS TEBs (noise equivalent difference in temperature requirement of 0.05 K at typical BT) [18]. On-orbit performance assessments indicate that the calibration uncertainty for this band is well within that specification [23]. Hence, numerous MODIS TEBs calibration performance assessments in the past have used this band as a reference.

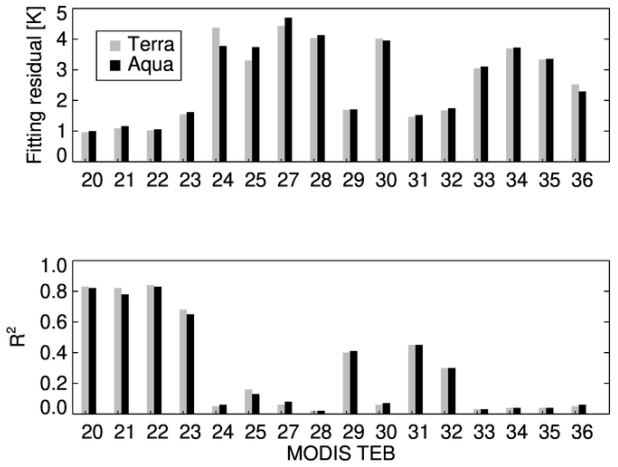

Fig. 4. (Top) Standard deviation of the absolute fitting residuals for the normalization technique over the ocean target for each TEB (using in situ SST as the reference measurement). (Bottom) Model's R^2 over the ocean target for each band. Only nighttime granules were used. Gray and black represent Terra and Aqua, respectively.

Because the fit's uncertainty (and association with the in situ SST) is band-dependent, the correlation and accuracy of the normalization technique can be evaluated using fitting residuals and the fit's R^2 [24]. Figure 4 displays the standard deviation (STD) of the absolute fitting residuals and R^2 for the normalization technique using the in situ SST as the reference measurement for both instruments and each TEB. Small STD values indicate a good fit, while large STD values denote scattering in the measurements around the model. As a form of cross-comparison and sanity check, Table I summarizes the fit's R^2 values using both the in situ SSTs and band 31 BTs as references for all the Terra and Aqua MODIS TEBs. An R^2 value close to 1 means highly correlated, while naught defines no correlation between the band's measurements and the reference data. Terra and Aqua MODIS show consistent results. Bands 20-23, 29, and 32 exhibit high correlation with band 31. With respect to the in situ SST, only bands 20-23 display high correlation, while bands 29 and 31 show reasonable association. Overall, the MWIR TEB BTs exhibit high dependency with the in situ SST, whereas the LWIR TEB display smaller correlation. On the other hand, all bands exhibit BTs reasonably correlated to those from band 31. This is expected, since all MODIS bands cover the same spatial resolution and use the same calibration algorithm. The idea of showing the model's performance for all bands is to demonstrate that the model works, but has its shortcomings, and be transparent just in case similar studies are performed where this method will be employed. Therefore, the results can be compared and used as a baseline. Moreover, the normalization method is mostly used to remove seasonal fluctuations in the data using the reference source. Hence, even if the reference does not correlate well with a particular channel, the trend can still be calculated, although it still contains a degree of seasonality, as a function of the reference. It is demonstrated in Section IV-A1 that the in situ SST and MODIS band 31 BT distributions over ocean vary monthly and induce asymmetrical artifacts to all TEB. Moreover, their monthly standard deviations are significantly affected by these asymmetrical features. Hence, by normalizing the ocean data, its distribution becomes symmetrical and near-Gaussian for most bands. Thus reducing the ocean fluctuation effects and, in turn, the measurement uncertainty. These improvements allow for feasible instrument performance assessments. Lastly, the goodness-of-fit is both scene- and band-dependent. However, this is just one metric that can be used to evaluate the improvements produced by the normalization method. More importantly, a major advantage when using a non-MODIS-related reference measurement is that this allows for the opportunity to evaluate all the MODIS data, since band 31 is not being used as the reference measurement. The normalization technique application to the MODIS data using both reference measurements (in situ and band 31) is discussed in Section IV-A1.

It is important to mention that the correlation between bands 31 and 32 and the in situ SST has more to do with the difference in fluctuations between these than an issue with the methodology. The model is not able to fully capture the fluctuations and normalize the data (to remove its seasonality) in these bands using the in situ SST. However, because MWIR bands 20-23 have an average BT closer to the average in situ SST (an important parameter in the normalization), and exhibit larger oscillations similar to those from the in situ SST, the model is better able to describe the behavior of these bands and

thus remove their seasonality. As mentioned previously, the main purpose of the model is to normalize the data to a reference source with the intention of removing large fluctuations. Afterwards, the normalized data is assessed for trends (Section IV-A2). Hence, a low correlation is mostly indicative of the fact that the seasonal fluctuations in the MODIS data will not be entirely removed. Moreover, as already discussed, using the in situ data allows for the evaluation of all bands. As opposed to using band 31 as the normalization reference. Furthermore, it is evident that all bands should somehow correlate to band 31, since all retrievals are performed over the same space (with matching resolution) and using the same calibration algorithm. Hence, using the ocean buoy data introduces an external source with which to evaluate all bands. Lastly, there will be limitations to the method, just like for most, but it can be a useful tool to standardize the satellite data and remove large variations, even if for some bands.

TABLE I
FITTING MODEL'S R^2 FOR ALL TERRA AND AQUA MODIS TEBS USING THE BAND 31 BTS AND IN SITU SSTS AS REFERENCE OVER THE OCEAN TARGET.

	R^2			
TEB	TERRA		AQUA	
	IN SITU	BAND 31	IN SITU	BAND 31
20	0.83	0.77	0.82	0.79
21	0.82	0.72	0.78	0.72
22	0.84	0.71	0.83	0.73
23	0.68	0.78	0.65	0.79
24	0.05	0.44	0.06	0.43
25	0.16	0.63	0.13	0.57
27	0.06	0.03	0.08	0.03
28	0.02	0.17	0.02	0.16
29	0.40	0.95	0.41	0.95
30	0.06	0.50	0.07	0.52
31	0.45	-	0.45	-
32	0.30	0.97	0.30	0.97
33	0.03	0.56	0.03	0.55
34	0.04	0.46	0.04	0.45
35	0.04	0.44	0.04	0.42
36	0.05	0.37	0.06	0.36

C. Spectral mismatch correction using MODTRAN

A typical radiance spectrum over an ocean target simulated using MODTRAN 5.0 was used to derive a correction for the relative spectral response (RSR) mismatch caused by spectral differences between some of the Terra and Aqua MODIS TEBs as well as variations in the columnar atmospheric water vapor content (Fig. 5). MODTRAN can provide the spectral signature of a typical tropical ocean target at a fine spectral resolution of 1 nm [25]. This high spectral resolution is vital when characterizing the impacts of various water vapor absorption features on the retrieved top-of-atmosphere radiance. Using the high-resolution spectral profile, a Spectral Band Adjustment Factor (SBAF) can be calculated as such:

$$SBAF = \frac{\int_{\lambda_1}^{\lambda_2} L_{MODTRAN} RSR_{Terra} d\lambda}{\int_{\lambda_1}^{\lambda_2} RSR_{Terra} d\lambda} \Bigg/ \frac{\int_{\lambda_1}^{\lambda_2} L_{MODTRAN} RSR_{Aqua} d\lambda}{\int_{\lambda_1}^{\lambda_2} RSR_{Aqua} d\lambda}, \quad (6)$$

where $L_{MODTRAN}$ is the hyperspectral profile simulated using MODTRAN, λ_1 and λ_2 denote the wavelength range of the spectral band, and RSR_{Terra} and RSR_{Aqua} define the RSRs for the TEB that is being spectrally-matched for Terra and Aqua MODIS, respectively. MODTRAN radiance profiles were simulated using data from the MODIS Atmospheric Profile product as input [26]. From this product, the parameters of interest were: layer elevation, layer pressure, layer water vapor mixing ratio, and layer temperature. All of these parameters are produced day and night at 5x5 1-km pixel resolution when at least 9 field-of-views are cloud free.

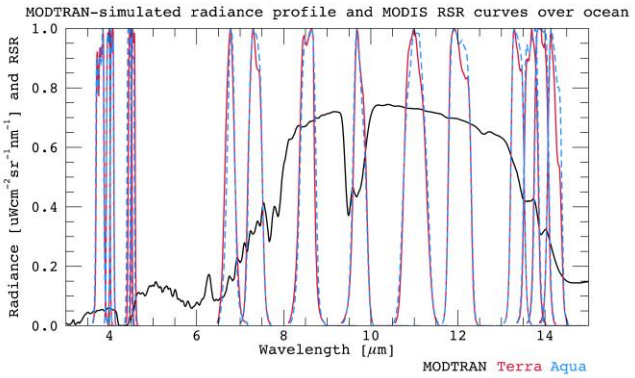

Fig. 5. MODTRAN profile over an ocean target simulated by using data from the MODIS Atmospheric Profile product as input. MODIS RSRs are superimposed over the MODTRAN simulation.

For this study, a 15 km x 15 km ROI surrounding the ocean site coordinates was selected, and the average value of these four parameters at every atmospheric layer was calculated for each MODIS granule coincident with the ocean target. Figure 6 illustrates the Terra MODIS mission-long atmospheric layer elevations, temperatures, water vapor mixing ratios, and pressures over the ocean target as obtained from the Atmospheric Profile product. Numerous studies have shown that the MODIS Atmospheric Profile product correlates quite well with both radiosonde and Global Positioning System measurements over Germany, Costa Rica, China, and the Iberian Peninsula, to name a few locations [27]-[30]. Moreover, it has been demonstrated that the MODIS Atmospheric Profile product provides similar results to those produced by satellite-derived profiles from the Atmospheric InfraRed Sounder and five reanalysis profiles (the European Centre for Medium-range Weather Forecasts (ECMWF), the Modern-Era Retrospective analysis for Research and Applications, Version 2 (MERRA2), the National Centers for Environmental Prediction (NCEP)/Global Forecasting System (GFS), NCEP/Final Operational Global Analysis (FNL), and NCEP/Department of Energy (DOE))[31]. Hence, while using the ECMWF profile

(or any other "external" source) makes logical sense because it does not come from MODIS, the analyses themselves will not change much, since the atmospheric transmittance, upwelling and downwelling radiances, and water vapor content are only slightly larger for MODIS when compared to ECMWF, and the impact caused by their differences on higher level products such as land surface temperature is smaller than 0.3 K.

Once the SBAF is computed for all the MODIS TEBs, it can be used to correct either the Terra or Aqua MODIS radiances as follows:

$$L_{MODIS_{corr}} = L_{MODIS} \times SBAF, \quad (7)$$

where L_{MODIS} is the Terra or Aqua MODIS radiance and $L_{MODIS_{corr}}$ is the radiance after being spectrally-corrected to match its equivalent Terra or Aqua MODIS band. In the case of this study, the SBAF were derived as Terra-to-Aqua ratios; meaning that you would apply the SBAF (Eq. (7)) to the Aqua radiances to correct them. Afterwards, the radiances can be converted to BTs using Planck's law. In this study, one-year data were used to produce band-dependent SBAF values for every MODIS granule available. Afterwards, these SBAF values were observed against time and found to be quite stable throughout the year. Hence, a constant SBAF value was used for each band. Moreover, even though the SBAF values are scene dependent, all MODIS data are overlooking roughly the same region-of-interest (20 km by 20 km) and one specific scene type (ocean; warm temperatures). Thus, providing further justification for the usage of constant values. The SBAF were applied before the normalization. The in situ SST were used to run the MODTRAN simulation. Lastly, using the mission-long $L_{MODTRAN}$ computed with the MODIS Atmospheric Profile product data as input, bands 31 and 32 were analyzed to make sure there are no water vapor-induced BT trends from years 2000 to 2020 over the ocean site. The BT difference between these two bands (BT_{31}-BT_{32}) is commonly used in a split-window algorithm to obtain water vapor. This split-window technique is widely used to retrieve the land surface temperature from satellite measurements [32]. Hence, atmospheric effects can be characterized based on the differential absorption between adjacent infrared bands. MODIS band 32 (12-μm) is more sensitive to atmospheric water vapor absorption than its adjacent MODIS band 31 (11-μm). The difference between the BT retrieved from these two bands is indicative of the atmospheric water vapor content. Thus, there is high correlation between BT_{31}-BT_{32} and water vapor. The MODTRAN-produced BTs indicate marginal trends for bands 31 (-0.10 K/yr) and 32 (-0.09 K/yr). Moreover, the difference (-0.01 K/yr) between these trends is negligible and indicative of no water vapor-produced trend over the site throughout the instrument's mission.

D. MODIS data at different AOIs

Generally, the MODIS BT trends at different AOIs are used to track its on-orbit RVS stability. Since the MODIS TEBs RVSs are normalized to the BB AOI, it is suitable to reference all BTs at different AOIs to the BT at the BB AOI, and define the BT difference, ΔT_{RVS}, at each AOI as:

$$\Delta T_{RVS} = [BT(AOI_i)] - [BT(AOI_{BB})] \; i = 0,1,2,3,\dots,N, \quad (8)$$

where N is the total number of AOIs designated between 10.5° and 65.5°. In this study, 13 evenly-spaced AOIs (14.5°, 18.6°, 22.6°, 26.7° (BB), 30.8°, 34.8°, 38.9°, 42.9°, 47.0°, 51.1°, 55.2°, 59.2°, 63.3°) were selected. Because there are roughly 2 overpasses for each MODIS instrument, it is possible that we won't have the whole AOI range with just a few weeks or months' worth of data. Therefore, all of the ΔT_{RVS} calculations are performed at the yearly level; meaning that we would look at whole years and bin the data using the 13 chosen AOIs by looking at 100 frames (roughly 4˚) to the left- and right-hand sides of the selected bin value accordingly. Hence, for each year of both MODIS missions, the data were divided into 13 AOI bins and each bin's average value was calculated. Afterwards, ΔT_{RVS} was computed. Prior to the binning process, all of the MODIS data will have been normalized using the technique described in Section III-A. Moreover, the data will also be normalized to the beginning of the mission (by subtracting to the first-year value of available data) in order to see the actual RVS trends for each TEB. This is discussed in Section IV.

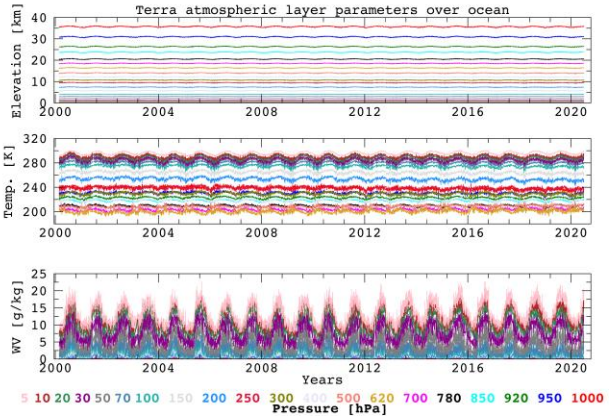

Fig. 6. Terra MODIS mission-long atmospheric layer elevations, temperatures, water vapor mixing ratios, and pressures over the ocean target as obtained from the Atmospheric Profile product.

IV. Results and Discussion

A. Stability assessments

1) SST as reference

As discussed in Section III-A, the normalization technique is applied to the MODIS data prior to all the calibration assessments. In this section, the normalization method application and subsequent stability assessment results are presented after normalizing each MODIS TEB's data to the in situ SSTs. Figure 7 illustrates the BTs as a function of the in situ SSTs, as well as the empirical model applied to Terra MODIS TEBs 23, 29, and 35. The empirical model presented in Eq. (4) is used to determine the dependency between the

MODIS band BTs using the in situ SSTs as reference. In this circumstance, the normalization BT is set to the average of the in situ SSTs over the entire Terra MODIS mission. The right panel charts display the probability distribution function (PDF) for each of these bands' BT range, and their PDF after the normalization is applied. Band 23 exhibits strong correlation with the in situ SSTs, and its PDF after normalization moved towards a Gaussian-shaped distribution. However, while there is some improvement after the normalization (narrower shape to its PDF) for band 29, it does not hold as good a correlation with the in situ SSTs as it does with band 31 (not shown). Band 35 exhibited close to no improvement.

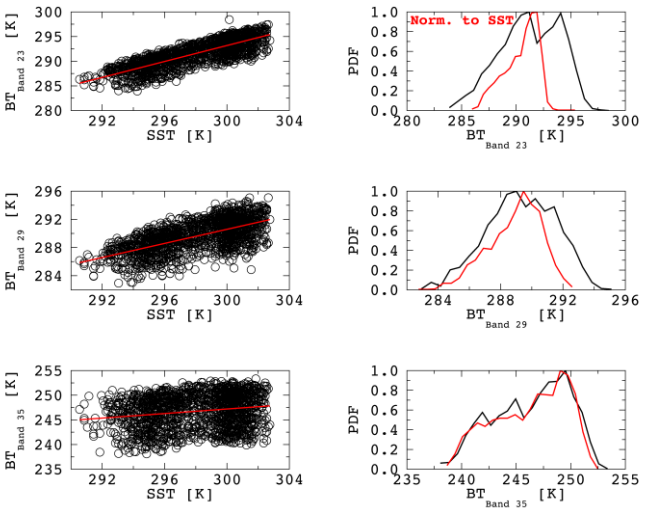

Fig. 7. (Left) Terra MODIS mission-long BTs as a function of in situ SSTs (black) and empirical model (red) for bands 23, 29, and 35 over the ocean target during nighttime. (Right) PDF for the selected MODIS TEBs BTs before (black) and after (red) the normalization technique has been applied.

Once the empirical model is derived, the normalization technique is then applied to the Terra and Aqua MODIS nighttime data to perform mission-long calibration stability assessments. In this section, we show an example of the normalization method being applied to Aqua MODIS bands 23, 29, and 35 in Figure 8. However, Section IV-A2 will discuss the trending results for all the MODIS TEBs for both instruments and cross-compare reference measurements (i.e. in situ SSTs *vs.* band 31 BTs). As mentioned in Section III-B, some bands' stabilities are BT-dependent. This is not surprising, as the normalization technique's accuracy is highly dependent upon the reference measurement. It is evident from Figure 8 that the seasonal variations have been removed from the Aqua MODIS mission-long BT trends for bands 23 and, to some extent, band 29 over the nighttime ocean measurements, while the band 35 BTs appear close to intact after the normalization. Removing the data's seasonality is beneficial, since this uncertainty can propagate to the long-term stability assessments. Data gaps in the "after normalization" trends are due to outages (non-functioning sensor or routine maintenance) in the buoy records, these non-data periods can be seen in Fig. 3. The trending results will be discussed in the next section.

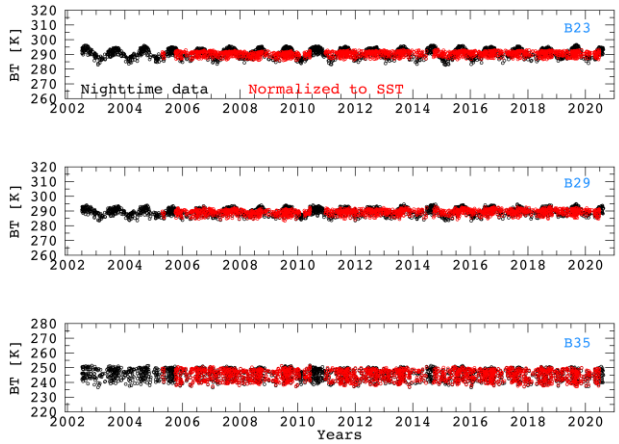

Fig. 8. Aqua MODIS mission-long BT trends for TEBs 23, 29, and 35 over the ocean site during nighttime. The black markers represent the ocean site MODIS BTs, while the red symbols define the MODIS BTs after being normalized using the in situ SSTs as reference.

2) Trends and reference measurements comparison

After the data was normalized for both MODIS instruments and all TEBs using both reference (in situ SSTs and band 31 BTs) measurements, yearly temperature trends were calculated. Table II summarizes the temperature change rates for all MODIS TEBs using both references. Overall, Terra MODIS band 30 exhibits the largest change rate (approximately -0.08 K/yr using either reference measurement). As stated earlier, the Terra PV LWIR bands are affected by electronic cross-talk, and its effect is characterized and corrected using lunar measurements in C6.1 [4]. Therefore, this downward trend may be partially due to some uncorrected cross-talk residuals during the cross-talk correction. Moreover, Aqua MODIS band 30 also displays a slight, downward trend of -0.028 and -0.012 K/yr using the band 31 BTs and the in situ SSTs, respectively. The cloud-top property and carbon dioxide bands 34 to 36 show approximately the same downward change rate for both instruments using either reference [33]. Additionally, atmospheric temperature bands 24 and 25, and cloud top altitude band 33, exhibit similar performance for both instruments and references. All other TEBs display stable trends (i.e. change rates smaller than 0.040 K/yr; which amounts to roughly 0.8 K for the entire mission).

As discoursed in other studies, some bands are affected by carbon dioxide (CO_2) absorption as the thermal radiation is transmitted through the atmosphere [34]-[36]. MODIS PC LWIR bands 33-36 undergo the most CO_2 absorption effects. As the CO_2 level increases, its absorption can cause the measurements from these bands to trend downward. One distinctive feature when using the in situ SST as the normalization reference is the fact that MODIS band 31 can be evaluated. Band 31 exhibits a negligible change rate of approximately 0.003 K/yr for both MODIS instruments; indicating that band 31 itself is well calibrated when evaluated with an external reference. Moreover, bands 20-23, all highly correlated with the in situ SST, have higher change rates (around 0.04 K/yr) when referenced to the in situ target, as

opposed to band 31 (roughly 0.01 K/yr); perhaps also indicative of some drifting for these bands.

Overall, previous literature does not include any calibration performance assessments using ocean data per se, but the MODIS C6.1 TEB on-orbit data's performance has been assessed over deep convective clouds (DCC), Dome-C, and via cross-comparison with Metop's IASI SNOs over different scene temperatures (which include ocean temperatures) [5],[8],[36]. All results show that Terra MODIS band 30 exhibits the largest (downward) trend with values of 0.19 K/yr, 0.11 K/yr, and 0.076 K/yr over DCC, Dome-C, and for SNOs (on average over typical temperatures), respectively. These results are quite similar to those shown in this study. This is a known issue for Terra MODIS C6.1. Moreover, atmospheric temperature bands 24 and 25, and cloud top altitude band 33 results over SNOs with typical temperatures exhibit similar performance to those over ocean (within 0.06 K/yr). All other bands display similar trends to those presented here. Conversely, Aqua MODIS band 30 does not exhibit such large drifts, but the 0.067 K/yr, 0.040 K/yr, and 0.036 K/yr downward trends over DCC, Dome-C, and SNOs with typical temperature scenes, correspondingly, are also comparable with the results revealed in this study. Likewise, all other Aqua MODIS bands exhibit similar trends to those demonstrated in these analyses.

TABLE II
MISSION-LONG BT CHANGE RATES FOR ALL TERRA AND AQUA MODIS TEBS OVER THE OCEAN SITE USING BOTH REFERENCE MEASUREMENTS.

	CHANGE RATE [K/YR]			
TEB	TERRA		AQUA	
	IN SITU	BAND 31	IN SITU	BAND 31
20	0.037	0.007	0.038	-0.003
21	0.037	0.0004	0.074	0.014
22	0.038	0.011	0.039	-0.005
23	0.037	0.009	0.038	-0.006
24	-0.037	-0.067	-0.033	-0.048
25	-0.005	-0.027	-0.000	-0.028
27	0.070	0.048	-0.031	-0.030
28	-0.016	-0.002	-0.007	-0.001
29	0.055	0.023	0.061	0.021
30	-0.076	-0.078	-0.012	-0.028
31	0.002	-	0.003	-
32	0.015	-0.002	0.029	0.001
33	-0.032	-0.037	-0.025	-0.042
34	-0.052	-0.055	-0.048	-0.061
35	-0.049	-0.053	-0.053	-0.062
36	-0.056	-0.049	-0.050	-0.048

B. Consistency assessment

After assessing the calibration stability for each MODIS instrument, the next step is to evaluate the consistency between them. Because Terra and Aqua MODIS have different overpass times over the site, the data can't be compared directly amongst days. Therefore, the mission-long nighttime data were monthly-averaged for both instruments, and the Terra minus Aqua difference for each month was calculated. This difference is referred to as the relative bias (RB). Figure 9 displays the mission-long RB trends for bands 23, 29, and 35 using the in situ SSTs as reference. Because, after carefully analyzing the results, we realized that the RB calculation values agreed quite well whether we used band 31 or the in situ target as references, and using the in situ SSTs allow for the evaluation of band 31, we only show the bias and trending results using the in situ SSTs as reference in Table III. Moreover, the results will include a comparison before and after the SBAF is applied for those bands with at least a 1% ratio difference between the Terra-to-Aqua MODTRAN simulated radiances (i.e. SBAF values ≥ 1.01).

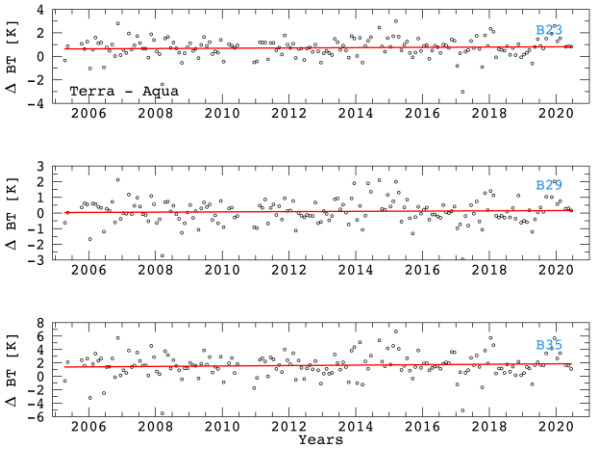

Fig. 9. MODIS mission-long RB trends for TEBs 23, 29, and 35 over the ocean site. Data are monthly-averaged. The black markers represent monthly data, while the red lines define the data's linear fit. All data have been normalized using the in situ SSTs as reference.

The results presented in Table III include the Mean Relative Bias (MRB), which itself is the average of the mission-long RB values, uncertainty, and change rates (yearly trends). Prior to applying the SBAF correction, it is evident that there are significant RSR differences between Terra and Aqua MODIS for bands 24, 25, 35, and 36. Bands 24 and 25 have a slight RSR shift between MODIS instruments. Previous radiative transfer modeling of this bandpass shift has demonstrated that Terra will characteristically be 4 K and 2 K higher than Aqua for bands 24 and 25, respectively. Moreover, some other differences over ocean sites have been proven to be attributable to atmospheric temperature sensitivity [13],[37]. These artifacts apply to bands 27, 28, and 30 as well. Nonetheless, all TEBs exhibit MRB values well within ±0.5 K, which is typically the criterion used to evaluate most bands. The MRB values for bands 24, 25, 35, and 36 were reduced drastically after the SBAF correction, particularly for bands 24 and 25 (from 7.19 K and 4.88 K to 0.09 K and 0.06 K, respectively). However, the SBAF correction appeared to increase the MRB values for bands 27 (0.20 K to 0.85 K) and 30 (-0.66 K to -1.20 K). This is perhaps ascribed to a significant increase in Terra MODIS electronic cross-talk between the PV LWIR bands after the safe mode event. MODIS C6.1 was implemented to correct this. However, while most of the electronic cross-talk impact was attenuated after the implementation of the new cross-talk correction

method, its remnants are well-characterized and documented [4]. An "after SBAF correction" MRB value of 0.72 K for band 35 may to related spectral and scan mirror characterization errors, and out-of-band (filter leaks) influences [38]. Lastly, bands 27 and 30 exhibit the largest change rates (0.112 K/yr and -0.035 K/yr, correspondingly) between Terra and Aqua MODIS, while all other bands indicate roughly a quite stable ±0.25 K Terra-to-Aqua drift.

TABLE III
MEAN RELATIVE BIAS, UNCERTAINTY, AND TRENDS FOR THE OCEAN SITE FOR ALL MODIS TEBS USING THE IN SITU REFERENCE.

TEB	MRB ± unc [K] No SBAF	MRB ± unc [K] SBAF	Trend [K/yr]
20	0.25 ± 0.30	-	0.008
21	-0.15 ± 0.53	-	-0.016
22	0.45 ± 0.37	-	0.011
23	0.32 ± 0.42	-	0.011
24	7.19 ± 1.51	0.09 ± 1.51	0.014
25	4.88 ± 1.15	0.06 ± 1.15	0.015
27	0.20 ± 2.26	0.85 ± 2.26	0.118
28	-0.01 ± 1.55	-	0.015
29	-0.02 ± 0.21	-	0.007
30	-0.66 ± 1.33	-1.20 ± 1.33	-0.035
31	-0.31 ± 0.37	-	0.001
32	0.08 ± 0.11	-	-0.002
33	0.45 ± 0.92	-	0.009
34	0.24 ± 1.31	-	0.012
35	1.47 ± 1.20	0.72 ± 1.20	0.016
36	1.87 ± 0.93	0.47 ± 0.93	0.004

C. RVS assessment

As previously discussed in Section III-D, the MODIS BT trends at different AOIs are used to track its on-orbit RVS stability. Moreover, because the MODIS TEBs RVSs are normalized to the BB AOI, it is appropriate to reference all BTs at different AOIs to the BB AOI BTs. The data shown in this section is normalized to the in situ SSTs and includes all MODIS overpasses to be able to cover all AOIs. Hence, in order to perform the RVS stability assessment, each year of data was binned in the 13 pre-selected AOIs and one average BT value per bin was obtained. Afterwards, for each year, the average BB AOI BT value was subtracted from every AOIs average bin value. Lastly, each AOIs time series was normalized to the value of the initial year (2006 in this case, since the in situ SST data started being recorded in 2005 and is incomplete) via subtraction. Figures 10 illustrates the time series for the 13 chosen AOIs for Terra and Aqua MODIS TEBs 23, 29, and 35 over the ocean target site. Overall, there appear to be no RVS drifts for these three bands. Sudden spikes in the times series are due to missing in situ SST data gaps (seen in Fig. 3 for years 2005, 2008, 2010, 2014, and 2019). This artifact causes sudden jumps in the yearly average data because months of data are missing. Moreover, both the MODIS and in situ SST data stop at August 31st, 2020. Some additional noise in band 23 can be due to the fact that MODIS MWIR TEBs 20-24 have strong seasonal fluctuations that occur at the sunglint region over the ocean for large AOIs due to solar radiation specular reflection [39],[40].

To provide deeper insight to the analysis and a better understanding of the results, the yearly data was fitted with a least-squares regression to track the MODIS TEBs RVSs long-term drifts. Afterwards, the fitted 2020 value was subtracted from the fitted 2006 value, and this was considered to be the RVS drift for each AOI and TEB. Tables IV and V summarize the RVS drifts for all Terra and Aqua MODIS TEBs and selected AOIs for the ocean target site. Overall, the RVS drifts demonstrate stable long-term trends that remain under the radiometric requirements (0.5 K) for most MODIS TEBs, with a few exceptions. Terra MODIS TEBs 25 and 27 exhibit the largest RVS drifts (-1.3 K and 1.3 K, respectively) at the either close-to- or edge-of-scan AOIs (14˚ and 18˚), but most Terra MODIS RVS drifts fall within ±0.5 K for all TEBs. Aqua MODIS TEBs 25 and 27 also display the largest RVS drifts (up to -1.9 K for both) at the edge-of-scan AOIs, while band 27 also exhibits some large drifts at the middle-of-scan AOIs. However, apart from the above-mentioned large RVS drifts for the middle-of-scan angle and expected drifts at the edge-of-scan AOIs, most Aqua MODIS TEBs and AOIs fall within ±0.5 K as well. Moreover, it can be inferred from Fig. 1 that the MODIS LWIR TEBs (27-36) display a larger response to the RVS. Generally, MODIS TEBs 27-36 displayed average RVS drifts close to or under their radiometric requirements (which cover from 0.27 K to 0.62 K for the MODIS LWIR TEBs) at typical radiance. These results are comparable to those obtained in previous literature [12]-[14]. These studies evaluated the MODIS on-orbit RVS performance over the ocean and Dome-C. The caveat being that two of these studies were performed for C6, while the only C6.1 RVS assessment was performed over Dome-C using a reference site (Automatic Weather Station). Furthermore, the assessments over ocean did not use a reference source to evaluate RVS performance. These two reasons are part of the motivation for our study. Overall, our results agree with those previously published for most bands (within 0.5 K and 1.2 K over ocean and Dome-C, respectively). Naturally, because of the electronic cross-talk effects on bands 27-30, and the fact that these artifacts are not corrected in C6, our results (C6.1) disagree (we show smaller biases) with those presented for the previous collection for these bands. Nonetheless, the conclusion is similar, no noticeable RVS changes for the MODIS TEB. While the unit of RVS is percent, the impact of RVS error on the TEB calibration varies with scene temperature. Thus, the motivation or idea behind expressing the impact in temperature units came from the fact that this study focuses on a specific scene type (ocean; warm temperatures), and we believed it would be useful for the reader to see the direct impact caused by RVS errors in temperature units when it comes to these specific scenes. Moreover, the uncertainties for the RVS drifts at each AOI in Tables IV and V help provide information if the observed RVS drifts are significant or not. Moreover, after the latest Terra MODIS DSM, Xiong *et al.* showed that the TEBs RVSs characterization changed marginally, and that the differences between the first (March 26th, 2003) and third (August 5th, 2017) pitch maneuvers are still within the accepted 0.2 % for all TEBs – except for TEBs 27-30 (not included in that study) and 31 (0.3 %) [41].

Lastly, we recognize other existing methodology to evaluate RVS using Observation-Background (O-B) BT biases at different AOIs (following techniques such as those applied by Chang Liu et al.) [33]. Using this method, the Background BTs can be simulated using radiative transfer models (RTMs) like the Community Radiative Transfer Model (CRTM) or MODTRAN, and atmospheric profile data as input. In this particular study, the intention is to evaluate any biases and RVS changes using an in situ (ocean buoy) source. There are two main reasons to advocate for this method, as opposed to using O-B BT biases, these are: (1) A direct comparison to a reference source is the most pure and straightest way to assess the stability of satellite retrievals. Using an O-B strategy, while still effective, makes more sense whenever there is a lack of ground truth data. Then we can perform RTM simulations for lack of another reference source. (2) Consistency. Sections IV-A1 and IV-A2 use the normalization strategy for all analyses, results, and discussions. Analyzing RVS changes using the O-B approach may add confusion to the content and flow of the paper; as it would move away from the methodology presented in this manuscript.

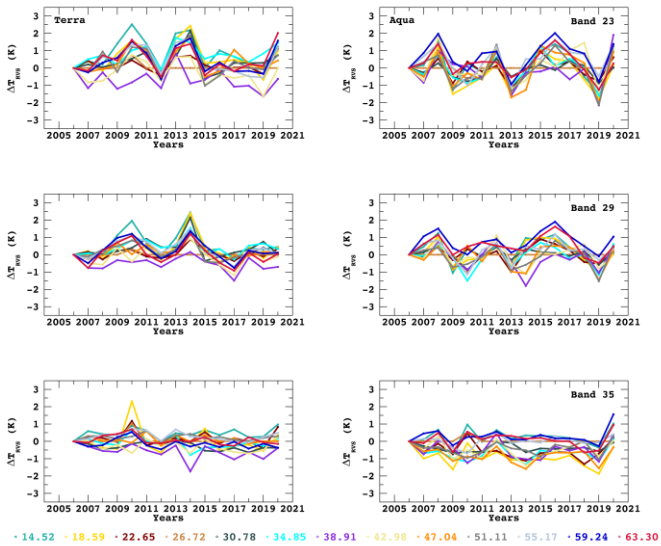

Fig. 10. Terra and Aqua MODIS time series for the 13 selected AOIs for bands 23, 29, and 35. The data shown is normalized to the in situ SSTs. Each year of data was binned in the 13 pre-selected AOIs and one average BT value per bin was obtained. Afterwards, for each year, the average BB AOI BT value was subtracted from every AOIs average bin value. Lastly, each AOIs time series was normalized to the value of the initial via subtraction.

TABLE IV
TERRA MISSION-LONG RVS DRIFT AND UNCERTAINTY FOR ALL TEBS AND SELECTED AOIS. UNITS ARE IN KELVIN.

AOI	TEB															
	20	21	22	23	24	25	27	28	29	30	31	32	33	34	35	36
14	-0.21 ± 0.82	-0.23 ± 0.80	-0.28 ± 0.79	-0.05 ± 0.87	0.03 ± 0.55	0.00 ± 0.80	0.55 ± 1.23	1.24 ± 1.22	-0.14 ± 0.75	0.12 ± 0.46	0.04 ± 0.69	0.23 ± 0.64	0.35 ± 0.37	0.44 ± 0.37	0.21 ± 0.28	-0.25 ± 0.30
18	0.00 ± 0.77	0.14 ± 0.81	0.00 ± 0.85	-0.05 ± 0.85	-0.40 ± 0.99	-0.13 ± 0.97	-1.33 ± 1.22	-0.33 ± 1.02	-0.02 ± 0.69	-0.28 ± 1.00	0.14 ± 0.65	0.20 ± 0.67	-0.02 ± 0.65	-0.12 ± 0.80	-0.26 ± 0.74	-0.37 ± 0.59
22	0.22 ± 0.29	0.28 ± 0.39	0.26 ± 0.41	0.18 ± 0.42	-0.10 ± 0.52	-0.02 ± 0.45	-0.11 ± 0.67	-0.15 ± 0.56	0.07 ± 0.31	0.28 ± 0.57	0.12 ± 0.28	0.02 ± 0.30	0.00 ± 0.35	0.00 ± 0.43	-0.02 ± 0.41	-0.01 ± 0.36
26	-0.05 ± 0.09	-0.05 ± 0.08	-0.08 ± 0.13	-0.11 ± 0.19	-0.21 ± 0.36	-0.19 ± 0.32	0.13 ± 0.23	0.14 ± 0.25	-0.05 ± 0.08	-0.03 ± 0.06	-0.12 ± 0.20	-0.11 ± 0.19	-0.15 ± 0.26	-0.18 ± 0.31	-0.16 ± 0.27	-0.09 ± 0.15
30	0.21 ± 0.59	0.23 ± 0.78	0.19 ± 0.78	0.20 ± 0.64	-0.26 ± 0.27	-0.22 ± 0.37	-1.28 ± 1.15	-0.55 ± 0.85	0.14 ± 0.59	-0.39 ± 0.43	0.12 ± 0.59	0.19 ± 0.50	-0.20 ± 0.29	-0.36 ± 0.28	-0.36 ± 0.22	-0.36 ± 0.21
34	0.91 ± 0.57	0.93 ± 0.73	0.87 ± 0.72	0.58 ± 0.55	-0.20 ± 0.52	0.15 ± 0.46	-1.35 ± 1.36	-0.62 ± 0.91	0.20 ± 0.45	-0.31 ± 0.50	0.18 ± 0.52	0.21 ± 0.48	-0.04 ± 0.35	-0.27 ± 0.40	-0.27 ± 0.34	-0.35 ± 0.23
38	0.05 ± 0.66	-0.03 ± 0.75	-0.20 ± 0.72	-0.44 ± 0.63	-1.00 ± 0.77	-0.64 ± 0.56	0.21 ± 1.43	0.60 ± 1.07	-0.33 ± 0.40	-0.65 ± 0.69	-0.28 ± 0.44	-0.28 ± 0.43	-0.01 ± 0.37	-0.49 ± 0.48	-0.56 ± 0.43	-0.61 ± 0.34
42	-0.71 ± 0.65	-0.85 ± 0.69	-0.97 ± 0.75	-0.50 ± 0.68	-0.49 ± 0.52	-0.51 ± 0.49	0.77 ± 1.64	1.29 ± 1.44	-0.19 ± 0.52	-0.28 ± 0.69	0.14 ± 0.55	-0.03 ± 0.50	0.19 ± 0.40	-0.03 ± 0.41	-0.20 ± 0.34	-0.28 ± 0.30
46	0.20 ± 0.73	-0.07 ± 0.78	-0.17 ± 0.82	0.16 ± 0.71	-0.36 ± 0.37	-0.21 ± 0.37	-0.32 ± 1.54	0.32 ± 1.36	-0.02 ± 0.41	-0.46 ± 0.46	0.20 ± 0.45	0.14 ± 0.41	-0.04 ± 0.27	-0.04 ± 0.30	-0.11 ± 0.22	0.02 ± 0.23
50	0.54 ± 1.04	-0.02 ± 1.02	-0.10 ± 1.02	-0.15 ± 0.82	-0.20 ± 0.31	-0.18 ± 0.53	-0.96 ± 1.42	-0.11 ± 1.04	-0.24 ± 0.49	-0.07 ± 0.56	-0.22 ± 0.55	-0.17 ± 0.43	-0.03 ± 0.31	-0.05 ± 0.24	-0.04 ± 0.17	-0.05 ± 0.19
54	-0.03 ± 0.96	-0.21 ± 0.89	-0.29 ± 0.93	-0.36 ± 0.79	-0.16 ± 0.46	-0.04 ± 0.71	-0.27 ± 1.40	0.51 ± 1.08	-0.25 ± 0.55	0.01 ± 0.66	-0.16 ± 0.57	0.04 ± 0.54	0.03 ± 0.36	0.00 ± 0.30	-0.11 ± 0.26	-0.24 ± 0.29
58	-0.22 ± 0.77	-0.12 ± 0.76	-0.13 ± 0.80	0.08 ± 0.79	-0.37 ± 0.43	-0.11 ± 0.70	0.06 ± 1.43	0.28 ± 1.15	-0.25 ± 0.59	-0.02 ± 0.48	-0.12 ± 0.60	0.08 ± 0.56	-0.08 ± 0.42	-0.13 ± 0.27	-0.29 ± 0.27	-0.29 ± 0.26
62	-0.30 ± 0.72	-0.19 ± 0.68	-0.15 ± 0.69	0.31 ± 0.77	-0.54 ± 0.45	-0.30 ± 0.75	0.51 ± 1.29	0.23 ± 0.94	-0.36 ± 0.61	-0.06 ± 0.66	-0.24 ± 0.63	-0.05 ± 0.59	-0.13 ± 0.48	-0.18 ± 0.31	-0.30 ± 0.26	-0.42 ± 0.20

TABLE V
AQUA MISSION-LONG RVS DRIFT AND UNCERTAINTY FOR ALL TEBS AND SELECTED AOIS. UNITS ARE IN KELVIN.

AOI	TEB															
	20	21	22	23	24	25	27	28	29	30	31	32	33	34	35	36
14	-0.23 ± 0.89	-0.10 ± 0.99	0.07 ± 0.93	-0.01 ± 0.95	0.36 ± 0.68	0.21 ± 0.80	-1.60 ± 1.42	-1.17 ± 0.88	-0.23 ± 0.71	0.10 ± 0.73	-0.14 ± 0.73	0.04 ± 0.71	-0.20 ± 0.54	0.09 ± 0.49	0.15 ± 0.47	0.02 ± 0.32
18	-0.12 ± 0.82	0.10 ± 0.94	0.11 ± 0.95	-0.05 ± 0.91	-0.45 ± 0.62	-0.55 ± 0.75	-1.91 ± 1.37	-1.90 ± 0.95	0.04 ± 0.68	-0.75 ± 0.67	0.06 ± 0.67	0.24 ± 0.66	-0.62 ± 0.55	-0.70 ± 0.59	-0.56 ± 0.52	-0.24 ± 0.33
22	0.19 ± 0.49	0.30 ± 0.58	0.30 ± 0.60	0.22 ± 0.60	-0.36 ± 0.54	-0.29 ± 0.60	-0.74 ± 0.52	-1.05 ± 0.51	0.09 ± 0.50	-0.25 ± 0.56	0.16 ± 0.46	0.20 ± 0.45	-0.40 ± 0.43	-0.50 ± 0.53	-0.45 ± 0.48	-0.16 ± 0.31
26	0.12 ± 0.20	0.13 ± 0.22	0.12 ± 0.21	0.10 ± 0.17	-0.02 ± 0.04	0.03 ± 0.06	-0.33 ± 0.57	0.17 ± 0.29	0.15 ± 0.25	0.08 ± 0.13	0.05 ± 0.08	0.06 ± 0.10	-0.05 ± 0.09	-0.01 ± 0.01	-0.08 ± 0.13	-0.05 ± 0.08
30	0.08 ± 0.41	0.21 ± 0.43	0.18 ± 0.45	0.11 ± 0.42	-0.09 ± 0.27	-0.21 ± 0.35	-0.43 ± 1.05	-0.18 ± 1.03	-0.05 ± 0.37	-0.32 ± 0.46	-0.19 ± 0.33	0.05 ± 0.29	-0.01 ± 0.27	0.06 ± 0.30	-0.03 ± 0.24	0.12 ± 0.21
34	0.26 ± 0.68	0.59 ± 0.81	0.49 ± 0.82	0.31 ± 0.83	-0.03 ± 0.51	0.16 ± 0.72	0.19 ± 1.21	-0.56 ± 1.04	0.11 ± 0.65	-0.01 ± 0.60	-0.20 ± 0.56	0.14 ± 0.52	-0.05 ± 0.47	0.18 ± 0.56	0.01 ± 0.44	0.23 ± 0.29
38	-0.45 ± 0.92	0.06 ± 1.05	0.06 ± 1.16	-0.18 ± 1.00	0.02 ± 0.68	0.18 ± 0.97	0.03 ± 1.74	-0.95 ± 1.21	-0.27 ± 0.71	-0.07 ± 0.65	-0.47 ± 0.54	-0.22 ± 0.53	-0.35 ± 0.52	0.05 ± 0.66	-0.10 ± 0.55	0.30 ± 0.32
42	0.11 ± 0.92	0.53 ± 0.96	0.49 ± 1.07	0.44 ± 0.99	0.01 ± 0.62	-0.03 ± 0.82	-0.88 ± 1.73	-1.61 ± 1.09	-0.12 ± 0.61	0.34 ± 0.57	0.05 ± 0.52	0.07 ± 0.49	-0.31 ± 0.51	-0.04 ± 0.55	-0.12 ± 0.49	0.28 ± 0.31
46	0.53 ± 1.06	0.53 ± 1.16	0.57 ± 1.15	0.34 ± 1.08	-0.19 ± 0.72	-0.32 ± 0.80	-1.03 ± 1.64	-1.41 ± 1.06	-0.14 ± 0.69	0.02 ± 0.57	-0.11 ± 0.67	-0.01 ± 0.62	-0.40 ± 0.53	-0.27 ± 0.53	-0.36 ± 0.46	0.09 ± 0.34
50	0.32 ± 1.11	0.37 ± 1.13	0.44± 1.13	0.11 ± 1.02	0.47 ± 0.67	0.26 ± 0.72	-1.10 ± 1.51	-1.59 ± 1.10	-0.09 ± 0.64	0.52 ± 0.63	-0.12 ± 0.57	-0.15 ± 0.51	-0.20 ± 0.42	0.07 ± 0.46	0.12 ± 0.39	0.41 ± 0.39
54	0.61 ± 0.96	0.77 ± 0.87	0.85 ± 0.90	0.56 ± 0.84	0.44 ± 0.43	0.38 ± 0.62	-0.86 ± 1.49	-1.83 ± 1.19	0.13 ± 0.60	0.34 ± 0.77	0.17 ± 0.46	0.07 ± 0.50	-0.27 ± 0.41	0.16 ± 0.42	0.21 ± 0.30	0.46 ± 0.29
58	0.40 ± 0.94	0.21 ± 0.89	0.22 ± 0.91	0.18 ± 0.89	0.47 ± 0.58	0.58 ± 0.64	-0.32 ± 0.87	-0.90 ± 0.84	0.23 ± 0.60	0.37 ± 0.64	0.13 ± 0.54	0.19 ± 0.48	0.19 ± 0.46	0.40 ± 0.52	0.25 ± 0.43	0.26 ± 0.35
62	-0.02 ± 0.73	-0.30 ± 0.76	-0.34 ± 0.77	-0.28 ± 0.73	0.03 ± 0.47	0.20 ± 0.66	-0.39 ± 0.54	-0.80 ± 0.85	-0.09 ± 0.56	0.15 ± 0.68	-0.24 ± 0.57	-0.15 ± 0.50	-0.11 ± 0.46	0.16 ± 0.49	-0.04 ± 0.44	-0.02 ± 0.28

V. SUMMARY

The Terra and Aqua MODIS sensors have been - and continue to be - cornerstones for the global monitoring of numerous Earth geophysical changes. While both instruments continue to provide reliable daily scientific measurements well past their designed lifetimes, it is crucial to monitor them for any long-term changes. In this study, an ocean surface site was used as reference to perform calibration, consistency, and RVS stability assessments on all the MODIS TEBs. Analyses were performed in which the MODIS data were normalized to the in situ SSTs using an empirical model. Additionally, the Terra and Aqua MODIS TEBs were evaluated for consistency, and a SBAF correction was applied to all Terra/Aqua MODIS band pairs with significant spectral differences. The SBAF values were derived using simulated radiances (obtained from MODTRAN) and the Terra and Aqua MODIS RSRs.

Most Terra and Aqua MODIS TEBs show mission-long stable trends. Terra band 30 shows the largest downward trend, while Aqua band 30 also displays a descending drift, albeit with a much lower change rate. This is consistent when using both band 31 and the in situ target as references. Terra MODIS band 30 undergoes larger electronic cross-talk effects when compared to the other PV LWIR bands. To this effect, cross-talk correction coefficients are derived from lunar observations, and the correction is applied to the BB calibration and Earth radiance retrievals in C6.1. However, cross-talk residuals remain. The bands with the largest CO_2 absorption effects also display consistent downward drifts and change rates over the ocean site for both Terra and Aqua MODIS. Bands 27 and 30 display the largest Terra-to-Aqua biases and trends after the SBAF correction, while bands 24 and 25 were significantly corrected after the spectral correction. The MODIS TEBs RVSs on-orbit performance was assessed for both MODIS instruments. Terra and Aqua MODIS bands 25 and 27 exhibit the largest RVS drifts consistently for the edge-of-scan angles. Overall, the MODIS TEBs are stable and consistent (between instruments); with close to no change to their RVSs. All EV trending techniques discussed in this manuscript can be applied to monitor the on-orbit performance of current and future sensors.

ACKNOWLEDGMENT

The authors would like to thank MCST members Amit Angal and Ashish Shrestha for their helpful recommendations and suggestions; these helped improve the manuscript quality.

REFERENCES

[1] X. Xiong, K. Chiang, J. Esposito, B. Guenther, and W. Barnes, "MODIS On-Orbit Calibration and Characterization," *Metrologia*, vol. 40, no. 1, pp. 89-92, 2003.

[2] K. Chiang and X. Xiong, "Pre-launch characterization of Aqua MODIS scan mirror response versus scan angle for thermal emissive bands," in *Proc. SPIE 6677, 66771J*, 2007.

[3] Chris Moeller, Richard Frey, Eva Borbas, W. Paul Menzel, Truman Wilson, Aisheng Wu, Xu Geng, "Improvements to Terra MODIS L1B, L2, and L3 science products through using crosstalk corrected L1B radiances," in *Proc. SPIE 10402, Earth Observing Systems XXII*, 104020O, 2017.

[4] T. Wilson, A. Wu, A. Shrestha, X. Geng, Z. Wang, C. Moeller, R. Frey, and X. Xiong, "Development and Implementation of an Electronic Crosstalk Correction for Bands 27–30 in Terra MODIS Collection 6," *Remote Sensing*, vol. 9, no. 6, pp. 569, 2017.

[5] Y. Li, A. Wu, and X. Xiong, "Assessment of MODIS collection 6.1 thermal emissive band calibration using hyperspectral IASI observations," *Proc. of SPIE - Sensors, Systems, and Next-Generation Satellites XXIV*, vol. 11530, pp. 1153019, 2020.

[6] T. Chang, X. Xiong, and A. Angal, "Terra and Aqua MODIS TEB intercomparison using Himawari-8/AHI as reference," *J. Appl. Rem. Sens.*, vol. 13, no. 1, 017501, February 7, 2019.

[7] B. N. Wenny, X. Xiong, X., and J. Dodd, "MODIS thermal emissive band calibration stability derived from surface targets," in *Proc. SPIE: Sensors, Systems, and Next-Generation Satellites XIII 7474*, 74740W, 2009.

[8] X. Xiong, A. Shrestha, and B. Wenny, "Assessments of MODIS thermal emissive bands on-orbit calibration performance using Dome C observations," *Proc. SPIE 10986, Algorithms, Technologies, and Applications for Multispectral and Hyperspectral Imagery XXV*, vol. 10986, pp. 1098605, 2019.

[9] T. Chang, X. Xiong, A. Shrestha, and C. Perez Diaz, "Methodology development for calibration assessment using quasi-deep convective clouds with application to Aqua MODIS TEB," *Earth and Space Science*, 7, e2019EA001055, 2020.

[10] X. Xiong, V. V. Salomonson, K. Chiang, A. Wu, B. W. Guenther, and W. Barnes, "On orbit characterization of RVS for MODIS thermal emissive bands," in *Proc SPIE 5652*, 210, 2004.

[11] X. Xiong, A. Wu, B. Guenther, and W.L. Barnes, "On-orbit Monitoring of MODIS Thermal Emissive Bands Response Versus Scan Angle," in *Proc. of SPIE - Sensors, Systems, and Next-Generation Satellites XI 6744*, 67441I, 2007.

[12] A. Wu, I. Chu, X. Xiong, "Tracking long-term stability of the response versus angle for the MODIS thermal emissive bands with observations over clear ocean," in *Proc. of SPIE - Sensors, Systems, and Next-Generation Satellites XIV 7826*, 78261Z, 2010.

[13] B. N. Wenny, A. Wu, S. Madhavan, and X. Xiong, "Evaluation of Terra and Aqua MODIS Thermal Emissive Band Response Versus Scan Angle," in *Proc. of SPIE - Earth Observing Systems XIX 9218*, 92181L, 2014.

[14] A. Shrestha and X. Xiong, "Tracking Long-term Stability of MODIS Thermal Emissive Bands Response Versus Scan Angle Using Dome C Observations," in *Proc. of SPIE - Algorithms, Technologies, and Applications for Multispectral and Hyperspectral Imagery XXV 10986*, 109861, 2019.

[15] W. Barnes, T. S. Pagano, and V. V. Salomonson, "Prelaunch characteristics of the moderate resolution imaging spectroradiometer (MODIS) on EOS-AM1," *IEEE Trans.Geosci. Rem. Sens.*, vol. 36, pp. 1088-1100, 1998.

[16] T. Chang, C. Perez Diaz, A. Shrestha, and X. Xiong, "Application of quasi-deep convective clouds method for MODIS and VIIRS TEB calibration assessments," in *Proc. SPIE 11501, Earth Observing Systems XXV*, 115010K, 2020.

[17] X. Xiong, J. Sun, X. Xie, W. L. Barnes and V. V. Salomonson, "On-Orbit Calibration and Performance of Aqua MODIS Reflective Solar Bands," in *IEEE Transactions on Geoscience and Remote Sensing*, vol. 48, no. 1, pp. 535-546, Jan. 2010, doi: 10.1109/TGRS.2009.2024307.

[18] X. Xiong et al., "Terra and Aqua MODIS Thermal Emissive Bands On-Orbit Calibration and Performance," in *IEEE Transactions on Geoscience and Remote Sensing*, vol. 53, no. 10, pp. 5709-5721, Oct. 2015, doi: 10.1109/TGRS.2015.2428198.

[19] B. Guenther, G. Godden, X. Xiong, E. Knight, S. Qiu, H. Montgomery, M. Hopkins, M. Khayat, and Z. Hao, "Prelaunch algorithm and data format for the level 1 calibration products for the EOS-AM1 Moderate Resolution Imaging Spectroradiometer (MODIS)," *IEEE Transaction on Geoscience and Remote Sensing*, vol. 36, no. 4, pp. 1142-1151, 1998.

[20] X. Xiong, K. Chiang, J. Sun, W.L. Barnes, B. Guenther, V.V. Salomonson, "NASA EOS Terra and Aqua MODIS on-orbit performance," *Advances in Space Research*, vol. 43, no. 3, pp. 413-422, 2009.

[21] *MODIS Level 1B Algorithm Theoretical Basis Document*, NASA Technical Document, MODIS Characterization Support Team, 2013.

[22] *Automated data quality control checks and procedures of the National Data Buoy Center*, NOAA Technical Report, National Data Buoy Center, 1995.

[23] X. Xiong, A. Angal, W. Barnes, H. Chen, V. Chiang, X. Geng, Y. Li, K. Twedt, Z. Wang, T. Wilson, and A. Wu, "Updates of MODIS on-orbit calibration uncertainty assessments," *Proc. SPIE 10402, Earth Observing Systems XXII*, 104020M, https://doi.org/10.1117/12.2276305, 2017.

[24] W. H. Press, B. P. Flannery, S. Teukolsky, and W. T. Vetterling. "Numerical Recipes in C: The Art of Scientific Computing", Cambridge University Press, 1992.

[25] A. Berk, P. Conforti, R. Kennett, T. Perkins, F. Hawes, and J. van den Bosch, "MODTRAN6: a major upgrade of the MODTRAN radiative transfer code," in *Proc. SPIE 9088, Algorithms and Technologies for Multispectral, Hyperspectral, and Ultraspectral Imagery XX*, 90880H, 2014.

[26] E. Borbas, et al., *MODIS Atmosphere L2 Atmosphere Profile Product. NASA MODIS Adaptive Processing System*, Goddard Space Flight Center, USA: http://dx.doi.org/10.5067/MODIS/MOD07_L2.061, 2015.

[27] Z. Li, J.-P., Muller, and P. Cross, "Comparison of precipitable water vapor derived from radiosonde, GPS, and Moderate-Resolution Imaging Spectroradiometer measurements," *J. Geophys. Res.*, 108, 4651, doi:10.1029/2003JD003372, D20, 2003.

[28] P. Campos-Arias, G. Esquivel-Hernández, J.F. Valverde-Calderón, S. Rodríguez-Rosales, J. Moya-Zamora, R. Sánchez-Murillo, and J. Boll, "GPS Precipitable Water Vapor Estimations over Costa Rica: A Comparison against Atmospheric Sounding and Moderate Resolution Imaging Spectrometer (MODIS)," *Climate*. vol. 7 no. 5(63). https://doi.org/10.3390/cli7050063, 2019.

[29] L. Hailei, T. Shihao, Z. Shenglan, and J. Hu, "Evaluation of MODIS water vapour products over China using radiosonde data," *International Journal of Remote Sensing*, vol. 36, no. 2, pp. 680-690, DOI: 10.1080/01431161.2014.999884, 2015.

[30] J. A. Sobrino, J. C. Jiménez-Muñoz, C. Mattar, and G. Sòria, "Evaluation of Terra/MODIS atmospheric profiles product (MOD07) over the Iberian Peninsula: a comparison with radiosonde stations," *International Journal of Digital Earth*, vol. 8, no. 10, pp. 771-783, DOI: 10.1080/17538947.2014.93697, 2015,

[31] J. Yang, S-B. Duan, X. Zhang, P. Wu, C. Huang, P. Leng, and M. Gao. "Evaluation of Seven Atmospheric Profiles from Reanalysis and Satellite-Derived Products: Implication for Single-Channel Land Surface Temperature Retrieval," *Remote Sensing*. vol. 12, no. 5(791). https://doi.org/10.3390/rs12050791, 2020.

[32] Z. Wan and J. Dozier, "A generalized split-window algorithm for retrieving land-surface temperature from space," in *IEEE Transactions on Geoscience and Remote*

Sensing, vol. 34, no. 4, pp. 892-905, July 1996, doi: 10.1109/36.508406.

[33] T. C. Liu, X. Xiong, X. Shao, Y. Chen, A. Wu, T. Chang, and A. Shrestha, "Long term stability monitoring of Aqua MODIS thermal emissive bands through radiative transfer modeling", in *Proceedings Volume 11501, Earth Observing Systems XXV*, 115011K, 2020.

[34] C. Moeller, H. E. Revercomb, S. A. Ackerman, W. P. Menzel, R. O. Knuteson, "Evaluation of MODIS thermal IR band L1B radiances during SAFARI 2000", *J. Geophys. Res.*, 108, 8494, 2003.

[35] C. Moeller, W. P. Menzel, and G. Quinn, "Review of Terra MODIS thermal emissive band L1B radiometric performance" in *Proceedings Volume 9218, Earth Observing Systems XIX*; 92180T, 2014.

[36] T. Chang, X. Xiong, and A. Shrestha, "Assessment of MODIS thermal emissive band calibration performance using deep convective clouds," *J. Appl. Remote Sens.*, vol. 13, issue 4, pp. 044526, 2019.

[37] S.W. Seemann and J. Li, "Operational Retrieval of Atmospheric Temperature, Moisture, and Ozone from MODIS Infrared Radiances," *J. Appl. Meteor.*, vol. 42, pp. 1072-1091, 2003.

[38] C. Moeller, S. Hook, D. Tobin, and V. Walden, "Assessing MODIS LWIR band calibration accuracy," in *Proc. SPIE 6296, Earth Observing Systems XI*, 62960B, September 7, 2006.

[39] S. M. Singh and G. Ferrier, "Observation of intense sun glint in 3.7 μm channel of the AVHRR," *Int. J. Remote Sens.*, vol. 18, pp. 3521-3533, 1997.

[40] A. Kumar, "Observations of intense sun glint in the daytime mid-infrared MODIS channels-feasibility for sea surface temperature retrievals," *Gayana*, vol. 68, no. 2, pp. 344-347, 2004.

[41] X. Xiong, A. Wu, A. Angal, K. Chiang, and J. Butler, "MODIS and VIIRS on-orbit calibration and characterization using observations from spacecraft pitch maneuvers," in *Proc. SPIE 10764, Earth Observing Systems XXIII*, 107640V, 2018.

Carlos L. Pérez Díaz is a senior research scientist with Science Systems and Applications, Inc. in Lanham, Maryland. He is both an MCST and VCST member at the NASA Goddard Space Flight Center.

Xiaoxiong Xiong received the B.S. degree in optical engineering from the Beijing Institute of Technology, Beijing, China, and the Ph.D. degree in physics from the University of Maryland at College Park, College Park, MD, USA.

He is currently an Optical Physicist with the NASA Goddard Space Flight Center, Greenbelt, MD, USA, where he is also the MODIS Project Scientist and the MODIS and VIIRS Calibration Scientist. In addition to remote sensing, he had also worked in the fields of optical instrumentation, nonlinear optics, laser/atomic spectroscopy, and mass spectrometry. See http://science.gsfc.nasa.gov/sed/bio/xiaoxiong.xiong-1 for more details.

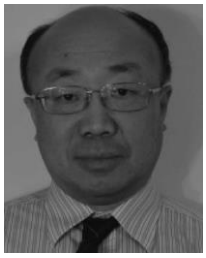

Aisheng Wu received the B.S. degree in atmospheric science from the University of Science and Technology of China, Hofei, China, the M.Sc. degree in atmospheric remote sensing from the Institute of Plateau Atmospheric Physics, Chinese Academy of Science, Lanzhou, China, and the Ph.D. degree in biometeorology/soil physics from the University of British Columbia, Vancouver, BC, Canada.

He is currently a Senior Scientist with MODIS and VIIRS Characterization and Support Teams and also with Sigma Space Corporation, Lanham, MD, USA.

Tiejun Chang received the M.S. degree in computer science from Montana State University, Bozeman, MT, USA, and the Ph.D. degree in optics from the University of Paris-Sud, Orsay, France.

He is currently with MODIS and JPSS VIIRS Characterization and Support Teams at the National Aeronautics and Space Administration, Goddard Space Flight Center in Greenbelt, MD, USA. He is involved in the radiometric calibration and validation of satellite remote sensors and has experience on MODIS, VIIRS, AVHRR, and GOES-R/ABI.